Electrical Power and Energy Systems 150 (2023) 109071

Contents lists available at ScienceDirect

International Journal of Electrical Power and Energy Systems

journal homepage: www.elsevier.com/locate/ijepes

Integrating degradation forecasting into distribution grids' advanced distribution management systems

Phuong H. Hoang [a,*], Gokhan Ozkan [b], Payam Ramezani Badr [c], Laxman Timilsina [c], Behnaz Papari [d,e], Christopher S. Edrington [c]

[a] Operation Technology Inc (ETAP), 17 Goodyear, Irvine, CA 92618, USA
[b] Dominion Energy Innovation Center, Holcombe Department of Electrical and Computer Engineering, Clemson University, North Charleston, SC 29405, USA
[c] Real-time Control and Optimization Laboratory, Holcombe Department of Electrical and Computer Engineering, Clemson University, Clemson, SC 29634, USA
[d] Holcombe Department of Electrical and Computer Engineering, Clemson University, Clemson, SC 29634, USA
[e] Department of Automotive Engineering, Clemson University, Greenville, SC 29607, USA

ARTICLE INFO

Keywords:
Distribution grids
Degradation forecasting
Advanced distribution management systems
Distributed energy resources
CHIL

ABSTRACT

Advanced distribution management systems (ADMSs) are considered tools for deploying control and management strategies to address challenges in future distribution grids populated with distributed energy resources (DERs). This work presents a framework to integrate a degradation forecasting (DF) layer into ADMSs. Based on observations of considered DERs' degradation behaviors, a load-dependent degradation model is constructed and integrated into a dynamical Markov chain-based degradation prediction model. Multiple sources of data can be used to train the Markov prediction model, and then Evidence Theory (ET) is used to fuse predicted results from the prediction model to enhance the reliability of the prediction model. Then, the predicted results are used to adjust energy management (EM), which is a component of the ADMS concept, to abate the degradation of components with higher degradation costs. The proposed strategy is verified on the IEEE 33 bus system by numerical simulations. In addition, controller-hardware-in-the-loop (CHIL) experimentation for the proposed scheme is implemented. Both the numerical simulations and CHIL experimentation show operation cost savings for the studied system.

1. Introduction

Distributed energy resources (DERs) are expected to be widely deployed in future distribution grids [1]. The integration of DERs will bring challenges for system control, management, and monitoring. To cope with the challenges, the future distribution grids will be given more autonomy in the form of digital control and management systems [1] to ease their control and management, and the advanced distribution management system (ADMS) concept is one of those [2]. With the dispersion of DERs, it is important to develop and integrate a degradation forecasting (DF) layer to ADMS to predict grid components' degradation behaviors to aid maintenance planning and real-time operation. Recently, DF for engineering systems has received growing interest because of the benefits of proper predictions of unpleasant events to take preventive actions [3–5]. However, DF is typically implemented for specific components, and there is a lack of frameworks to integrate DF into real-time control and management.

An ADMS is a software platform that provides a set of functions [6]. In the literature, a three-layer ADMS architecture consisting of device-level control (DLC), power management (PM), and energy management (EM) is proposed [7]. DLC, PM, and EM are also called the primary control layer, secondary control layer, and tertiary control layer, respectively [8]. The underlying idea of the multi-layer architecture is taking advantage of different time steps of the layers as upper layers have the duties of providing commands to lower layers. This architecture has been used in both alternating current (AC) and direct current (DC) grids; however, depending on the type of grid, quantities of interest are controlled and optimized.

EM has been extensively studied for electrical systems, including MW-scale systems like terrestrial power systems and ship power systems, as well as kW-scale systems like electrified vehicles' powertrain systems. EM is expected to be a key component of ADMS in future distribution grids, with the goal of cost savings. To achieve this goal, EM involves solving a well-defined optimization problem to find optimal energy allocation for different energy sources. EM's outputs are passed down to lower control layers as references for control activities, deciding the operating conditions for each energy conversion unit.

It has been reported in the literature that the operating conditions of energy conversion units affect their degradation rate [9–12]; thus,

* Corresponding author.
E-mail address: phuong.hoang@etap.com (P.H. Hoang).

https://doi.org/10.1016/j.ijepes.2023.109071
Received 8 June 2022; Received in revised form 18 December 2022; Accepted 26 February 2023
Available online 10 March 2023
0142-0615/

Nomenclature

ADMS	Advanced distribution management system
CAPEX	Capital expenditure
CHIL	Controller-hardware-in-the-loop
DER	Distributed energy resource
DF	Degradation forecasting
DFAF	Degradation forecasting & abatement framework
EM	Energy management
ET	Evidence Theory
MT	Microturbine
PM	Power management
PV	Photovoltaic
WT	Wind turbine
$P_n^D(Q_n^D)$	Active (Reactive) power generated by dispatchable source at bus n
Δt	Degradation forecasting sampling time
$\boldsymbol{\Pi}$	Markov transition matrix
λ_{ij}	Degradation intensity from state i to state j
$\mathbf{x}_n$	Vector of probabilities of the states of component at bus n, i.e., $\mathbf{x}_n = [x_{n,1}, x_{n,2}, x_{n,3}, x_{n,4}]$
$\mathcal{D}$	Set of buses which have a dispatchable energy source
$\overline{P_{n,i}^D}$	Maximum capacity of dispatchable energy conversion unit at bus n when it is in state i
$\overline{\lambda}$	Maximum degradation intensity matrix
$\overline{\lambda_{ij}}$	Maximum degradation intensity from state i to state j
π_{ij}	Transition probability from state i to state j
$\underline{\lambda}$	Minimum degradation intensity matrix
$\underline{\lambda_{ij}}$	Minimum degradation intensity from state i to state j
$d_n^e(d_n^a)$	Estimated (Actual) degradation signal of energy conversion unit at bus n
f_n^{eco}	Economic curve of dispatchable energy source at bus n
i, j	State index of a component
n, m	Bus index
t	Continuous time instant
t_k	Discrete time instant
$x_{n,i}$	Probability the component at bus n is at state i

degradation models should consider the operating conditions of components. Based on the role of EM in deciding operating conditions, EM can be used to prevent or reduce the degradation of components. Therefore, EM can be considered a means to prevent or reduce the degradation of components.

Quantifying uncertainty in DF is a challenging task. Degradation data is scarce because generating degradation data is challenging, costly, and time-consuming. Additionally, degradation data is often kept confidential by many involved parties, such as utilities and manufacturers. There are works that take the historical data of degradation signals to predict its future values by data-driven methods, for example, linear regression [13], Gaussian process regression [14]. However, the degradation process of a component is complex as it depends on its current state and future operating conditions. Furthermore, there are works that utilize deep neural network methods for degradation forecasting [15]. Due to the scarcity of degradation data, it is challenging to have sufficient information to construct a statistical model that can accurately predict future degradation behaviors and optimize real-time operation and maintenance planning. As a result, methodologies that combine multiple sources of information to arrive at a more informative piece with higher confidence are often used. There are works that integrate expert knowledge in degradation prediction to enhance forecasting performance. In fact, the Watchdog Agent intelligent maintenance system [16] uses sensed data, expert knowledge, and knowledge of engineering models.

Statement of Contributions: The main contributions of this paper can be summarized as follows. First, a Markov chain-based DF model is introduced to predict degradation paths of a grid's components in which components' states are modeled by a multi-state model. The model is a load-dependent model reasoning from observations of degradation behaviors of interested energy conversion units. Because degradation data is typically scarce, multiple sources of information are used to enhance the reliability of the prediction, and Evidence Theory's (ET) combination rule [12] is used to fuse multiple sources of data. The predicted results can aid maintenance planning and real-time operation. Second, this work focuses on the real-time aspect that a degradation abatement strategy for grid components is proposed in which the DF layer is integrated into the existing hierarchical ADMS as an upper layer to EM as illustrated in Fig. 1. The DF's predicted results are used to adjust EM's optimization problem to abate the degradation of higher degradation cost components. In addition to distribution grids, the proposed strategy can be applied to other applications. In [17], the proposed concept is used in DC microgrids in which the loss of load probability is the objective, while in this paper, the objective is the total degradation cost of the system. In [18], the proposed strategy is integrated into the EM of hybrid electric vehicles (HEVs). This work is a leverage of the two mentioned conference papers that, in addition to numerical simulations, controller-hardware-in-the-loop (CHIL) experimentation is carried out to show the cost-saving benefits of the proposed strategy.

The remainder of this paper is organized as follows. Section 2 formulates the problem and motivation for our approach. The DFAF is presented in Section 3. The proposed framework is validated in Section 4 by numerical simulations. Section 5 shows a CHIL experimentation for the proposed strategy. Section 6 ends this paper with a conclusion and future work.

2. Problem formulation

Consider a grid-connected distribution network consisting of multiple heterogeneous DERs dispersed over the network. As the granularity, a DER unit or a substation transformer is considered as a component in our work. Let $\mathcal{N} = \{1, \ldots, N\}$ be the set of all buses. The bus connecting directly with the substation is indexed 1. Sources supplying energy for the network can be categorized into dispatchable sources and non-dispatchable sources. Examples of dispatchable sources are microturbines (MTs) and substation transformers, and examples of non-dispatchable sources are wind turbines (WTs) and photovoltaic (PV) systems. Let $\mathcal{D}$ be the set of buses which have a dispatchable energy source.

Let P_n^D and Q_n^D be active and reactive power generated or delivered by a dispatchable source connected to bus n. Furthermore, active and reactive power generated by a non-dispatchable source at bus n are P_n^{ND} and Q_n^{ND}, respectively. Let $\mathbf{P}^D$ and $\mathbf{Q}^D$ be the vectors of active power and reactive power of all dispatchable energy sources, including the substation transformer, respectively. In addition, let $\mathbf{P}^{ND}$ and $\mathbf{Q}^{ND}$ accordingly be the vectors of active power and reactive power of all non-dispatchable DERs. Let V_n be the complex bus voltage at bus n. Denote $\mathbf{V} = [V_1, \ldots, V_N]^T$.

The primary function of EM is to optimally allocate power generation and delivery to sources of energy to gain economic objectives while adhering to system constraints [19–25]. Assume the DERs are

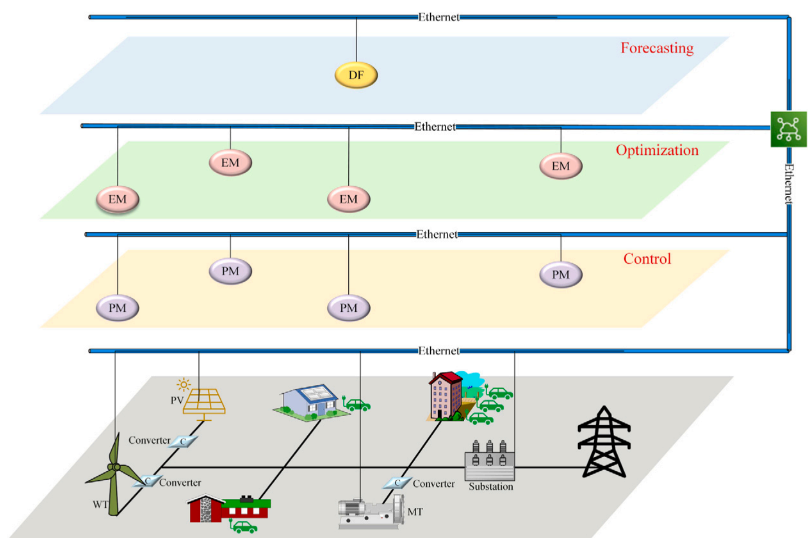

Fig. 1. ADMS with DF functionality.

allowed to participate in reactive power support to the network. EM takes predicted load and non-dispatchable active power generation information as inputs for its optimization process to output active power references for PM of dispatchable sources. Non-dispatchable active power generation of DERs like WTs and PVs can be estimated from weather information and their systems' models. With this setup, EM's optimization problem can be generally stated as

$$\min f^{eco}(\mathbf{P}^D) = \sum_{n \in D} f_n^{eco}(P_n^D) \tag{1a}$$

$$s.t.\ \mathbf{P}^D \in C^{\mathbf{P}^D}, \mathbf{Q}^D \in C^{\mathbf{Q}^D}, \tag{1b}$$

$$\mathbf{P}^{ND} \in C^{\mathbf{P}^{ND}}, \mathbf{Q}^{ND} \in C^{\mathbf{Q}^{ND}} \tag{1c}$$

$$\mathbf{V} \in C^{\mathbf{V}} \tag{1d}$$

where $C^{\mathbf{P}^D}$, $C^{\mathbf{Q}^D}$, $C^{\mathbf{P}^{ND}}$, $C^{\mathbf{Q}^{ND}}$, and $C^{\mathbf{V}}$ are the constraint sets of $\mathbf{P}^D$, $\mathbf{Q}^D$, $\mathbf{P}^{ND}$, $\mathbf{Q}^{ND}$, and $\mathbf{V}$, respectively. It is noted that all variables of the problem (1) can be transformed to bus voltages [26]. Conventionally, the objective function $f_n^{eco}(P_n^D)$ of energy source at bus n only considers economic curves of energy sources. That is, $f_n^{eco}(P_n^D)$ is the cost of buying electricity from the main grid if bus n connects with the substation transformer, and it is the fuel consumption cost if bus n connects with a fuel-based energy conversion unit.

After discussing the EM's optimization problem, the following observations can be obtained:

- Observation 1: EM decides operating conditions for the dispatchable source components as it outputs power references for lower layers to control the components to follow the references.
- Observation 2: It has been reported in the literature that the operating conditions of an energy conversion unit impact its degradation process that the higher the load, the higher the degradation rate, for example, gas turbines [27].

Components degrade over time, leading to the reduction of their values. In addition, different components may have different degradation rates and capital expenditures (CAPEX). Therefore, degradation costs should be taken into account along with the economic curves of components in the optimization process of the operation cost. With these above observations, EM can be considered as a means to adjust the degradation processes of the components in the system while still meeting customers' load demands. In the next section, a DFAF is proposed. First, it predicts the degradation paths of the components, and then the predicted results are used to reconfigure the EM's optimization problem to obtain optimal operation costs with degradation costs taken into consideration.

3. Degradation forecasting and abatement framework

This section presents a degradation forecasting and abatement framework. For the sake of completeness, some parts of [17,18] are presented in this work. However, compared to [17,18], this work is leveraged. First, the proposed strategy is discussed in a more detailed manner. Second, the objective of the proposed strategy is to reduce the total degradation costs.

3.1. Degradation model of components

3.1.1. Multi-state degradation representation

The binary model, which represents a system as either a failing or working state, is commonly used to model the state of a system due to its simplicity and computational efficiency. However, the multi-state model, which increases the granularity of the binary model, is often used in order to provide a more accurate representation of the system. A model with 4 states is often selected as a compromise between precision and complexity, as increasing the number of states can increase the complexity and computational burden of the model. For example, the authors in [28] describe a component using 4 states: perfect, useful, pseudo-fault, and fault. Similarly, the authors in [29] represent a coal-fired generating unit using 4 states, which are denoted by the numbers $1, 2, 3, 4$, based on its available generation capacity ranging from zero to its original maximum capacity. In [30], the state of drivetrain components of wind turbines is represented by normal working, degraded, critical, and functional failure states. Additionally, in [31], transformers are described using 4 states: good, fair, poor, and very poor.

The advancements in sensor technologies, industrial networks, and the semiconductor industry enables the deployment of online health monitoring for engineering systems to aid operation and maintenance planning, for instance, transformers [31], gas turbines [32], PV systems [3], and wind turbines [33]. Although different technologies may have different real-time health monitoring methodologies and configurations, there is a common process that data sensed by sensors are processed, and then they are input to degradation estimation engines to output degradation signals which are numerically represented and typically normalized [3,4,31,34,35]. By way of examples, for the case of generating units, the degradation signals typically are the performance ratio such as gas turbines [34], wind turbines [4], and PVs [35,36]. Denote $d_n^e(t_k)$ as the degradation signal of the component at bus n which is estimated at time t_k. The estimation of degradation signals is generally not a deterministic process. Therefore, it is assumed that the estimation has uncertainty that $d_n^e(t_k)$ is a sum of the actual degradation $d_n^a(t_k)$ and the error of the estimation $\sigma_n(t_k)$ as:

$$d_n^e(t_k) = d_n^a(t_k) + \sigma_n(t_k) \tag{2}$$

It is reasonable to assume that the degradation of a component has no improvement between two consecutive maintenance or repair times. The assumptions on degradation signals are formally stated as

Assumption 3.1.

(a) The maximum of the actual degradation $d_n^a(t)$ is 1.
(b) The actual degradation $d_n^a(t)$ is monotonically decreasing between two consecutive maintenance or repair times.

In [31], the authors convert degradation signals into 4 states by assigning each state in an interval. This work uses 4 states named by numbers from 1 to 4 and each state has a maximum capacity representation as the authors in [29] do. Also, the conversion from degradation signals to states are defined as

- State 1: In this state, the hard constraint for this state is $d_n^a \geq \rho_1$. The maximum capacity representation for this state is $\overline{P_{n,1}^D}$ and $\overline{P_{n,1}^{ND}}$ for dispatchable and non-dispatchable sources, respectively.
- State 2: In this state, the hard constraint for this state are $\rho_1 > d_n^a \geq \rho_2$. The maximum capacity representation for this state is $\overline{P_{n,2}^D}$ and $\overline{P_{n,2}^{ND}}$ for dispatchable and non-dispatchable sources, respectively.
- State 3: In this state, the hard constraint for this state are $\rho_2 > d_n^a \geq \rho_3$. The maximum capacity representation for this state is $\overline{P_{n,3}^D}$ and $\overline{P_{n,3}^{ND}}$ for dispatchable and non-dispatchable sources, respectively.
- State 4: In this state, the hard constraint for this state are $\rho_3 > d_n^a$. The maximum capacity representation for this state is $\overline{P_{n,4}^D}$ and $\overline{P_{n,4}^{ND}}$ for dispatchable and non-dispatchable sources, respectively. When a component enters this state, it is either considered not functional or required maintenance or replacement.

3.1.2. Markov chain based degradation model

There are works that take the historical data of $d_n^e(t)$ to predict its future values by data-driven methods, for example, linear regression [13], Gaussian process regression [14]. However, the degradation process of a component is complex as it depends not only on its current state but also on future operating conditions. In this work, a Markov chain-based degradation model is used to model the degradation process of a component. The model considers future operating conditions.

Denote $x_{n,i}$ as the probability that the component at bus n is at state i, $i \in \{1,2,3,4\}$, and $\mathbf{x}_n$ is the vector of all $x_{n,i}$, i.e., $\mathbf{x}_n = [x_{n,1}, x_{n,2}, x_{n,3}, x_{n,4}]$. The Markov model, illustrated in Fig. 2 (b), transitioning $\mathbf{x}_n$ at time t_k to $\mathbf{x}_n$ at time t_{k+1} has the following formula:

$$\mathbf{x}_n(t_{k+1}) = \mathbf{x}_n(t_k)\boldsymbol{\Pi} \tag{3}$$

where $\boldsymbol{\Pi}$ is the transition matrix

$$\boldsymbol{\Pi} = \begin{bmatrix} \pi_{11} & \pi_{12} & \pi_{13} & \pi_{14} \\ \pi_{21} & \pi_{22} & \pi_{23} & \pi_{24} \\ \pi_{31} & \pi_{32} & \pi_{33} & \pi_{34} \\ \pi_{41} & \pi_{42} & \pi_{43} & \pi_{44} \end{bmatrix} \tag{4}$$

Next, the derivation of the transition matrix is discussed. Because the model is to aid decision makings on operation and maintenance strategies, maintenance and repair are not considered in the model. The exponential distribution is typically assumed for the sojourn time in a state [28,37]. Let λ_{ij} be the degradation rate from state i to state j, $i \neq j$. It is noted that if the binary model is used, the degradation rate is the failure rate. Fig. 2 (a) is the state space diagram of the degradation rate.

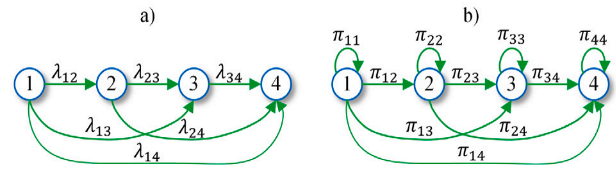

Fig. 2. Illustration of Markov chain model: (a) State space diagram of degradation rates, and (b) Markov model transition diagram.

Looking at the inflow and outflow of state i in the figure, the following equation can be derived:

$$\frac{dx_{n,i}(t)}{dt} = -x_{n,i}(t)\sum_{j=i+1}^{4}\lambda_{ij} + \sum_{j=1}^{i-1}x_{n,j}(t)\lambda_{ji} \tag{5}$$

In (5), it can be understood that the term $x_{n,i}(t)\sum_{j=i+1}^{4}\lambda_{ij}$ is the intensity of transitioning from state i to the other states. Additionally, the term $\sum_{j=1}^{i-1}x_{n,j}(t)\lambda_{ji}$ is the intensity of transitioning to state i from the other states. Solve (5) and discretize the solutions with sampling time Δt, the following equation can be obtained [17]

$$\pi_{11} = e^{-(\lambda_{14}+\lambda_{13}+\lambda_{12})\Delta t} \tag{6a}$$

$$\pi_{12} = \frac{\lambda_{12}}{\lambda_{14}+\lambda_{13}+\lambda_{12}}(1 - e^{-(\lambda_{14}+\lambda_{13}+\lambda_{12})\Delta t}) \tag{6b}$$

$$\pi_{13} = \frac{\lambda_{13}}{\lambda_{14}+\lambda_{13}+\lambda_{12}}(1 - e^{-(\lambda_{14}+\lambda_{13}+\lambda_{12})\Delta t}) \tag{6c}$$

$$\pi_{14} = \frac{\lambda_{1,4}}{\lambda_{1,4}+\lambda_{13}+\lambda_{12}}(1 - e^{-(\lambda_{14}+\lambda_{13}+\lambda_{12})\Delta t}) \tag{6d}$$

$$\pi_{21} = 0 \tag{6e}$$

$$\pi_{22} = e^{-(\lambda_{23}+\lambda_{24})\Delta t} \tag{6f}$$

$$\pi_{23} = \frac{\lambda_{23}}{\lambda_{23}+\lambda_{24}}(1 - e^{-(\lambda_{23}+\lambda_{24})\Delta t}) \tag{6g}$$

$$\pi_{24} = \frac{\lambda_{24}}{\lambda_{23}+\lambda_{24}}(1 - e^{-(\lambda_{23}+\lambda_{24})\Delta t}) \tag{6h}$$

$$\pi_{31} = 0 \tag{6i}$$

$$\pi_{32} = 0 \tag{6j}$$

$$\pi_{33} = e^{-\lambda_{34}\Delta t} \tag{6k}$$

$$\pi_{34} = 1 - e^{-\lambda_{34}\Delta t} \tag{6l}$$

$$\pi_{41} = 0 \tag{6m}$$

$$\pi_{42} = 0 \tag{6n}$$

$$\pi_{43} = 0 \tag{6o}$$

$$\pi_{44} = 1 \tag{6p}$$

The assumption that an energy conversion unit has a degradation rate depending on its operating conditions is reasonable. The thermal aspects is one of the main reasons for this assumption: Increasing power generation or transfer is likely to increase its operating temperature, and therefore it increases the degradation rate because of thermal effects, which is described by the exponential relation [9,10]. In this work, the relation between the degradation rate and power that a component generates and transfers P is modeled in (7). Particularly, a component has a constant degradation rate when its load is less than or equal to P^{norm}, but it exponentially increases when its load exceeds P^{norm}. This is because it is assumed that the operating temperature starts increasing exponentially at this point. With the deployment of EM, P is controlled to be less than its maximum capacity $\overline{P}$. Let λ_{ij} be the degradation rate when the component works in the region $P < P^{norm}$ and $\overline{\lambda_{ij}}$ when the component works at $\overline{P}$. The degradation rate when the component works in $[P^{norm}, \overline{P}]$ [17]:

$$\lambda_{ij} = \eta e^{\zeta P} \tag{7}$$

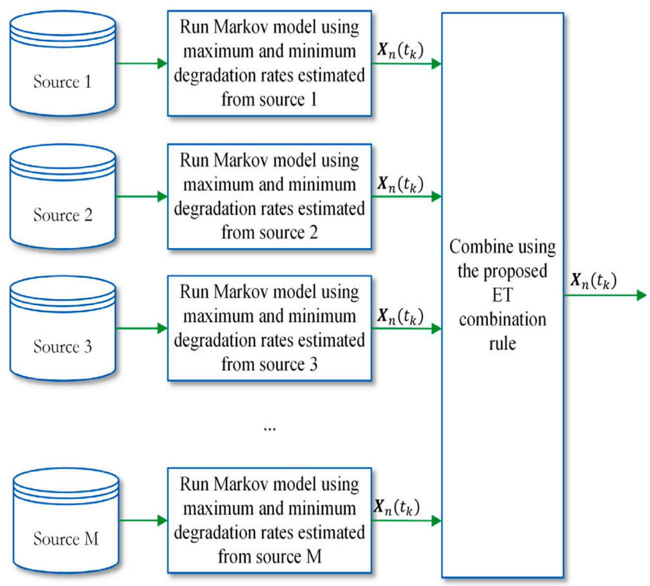

Fig. 3. Combining multiple sources of information using ET.

where

$$\zeta = \frac{\ln(\lambda_{ij}/\overline{\lambda_{ij}})}{P^{norm} - \overline{P}} \tag{8a}$$

$$\eta = \frac{\lambda_{ij}}{e^{\zeta P^{norm}}}. \tag{8b}$$

3.2. Combine multiple sources of information

The degradation rate model expressed in (7) in which $\overline{\lambda_{ij}}$ is understood as the maximum degradation rate and λ_{ij} is the minimum degradation rate. Three are many sources used to estimate the two parameters, for example, (1) field data, (2) accelerated testing data, (3) data provided by manufacturers, and (4) expert opinion.

The model (7) is sensitive the parameters $\overline{\lambda_{ij}}$ and λ_{ij}. If a single source of information is used and the source is not reliable, the model may not provide accurate results to aid decision makings. Hence, multiple sources of information are used. Particularly, each source of information, such as field data, manufacturers' data, is used independently to estimate $\overline{\lambda_{ij}}$, and λ_{ij} to run the Markov model. The results of running the Markov model are used to fuse using ET [12,38]. The combination is illustrated in Fig. 3.

3.3. Maximum capacity expectation degradation

A quantity to measure the degradation of a component's generation capacity is introduced in this section. Let $\mathbb{P}_n^D(t_k)$ be the maximum capacity expectation at time t_k of a dispatchable-source component. The maximum capacity expectation of a dispatchable source at bus n at time t_k is the maximum capacity that it is expected to be able to generate, and it has the following formula

$$\mathbb{P}_n^D(t_k) = \mathbb{E}(\overline{P_n^D}) = \sum_{i=1}^{4} x_{n,i}(t_k)\overline{P_{n,i}^D} \tag{9}$$

where $\mathbb{E}$ is the expectation operator. For non-dispatchable DERs, the maximum capacity expectation is similar as

$$\mathbb{P}_n^{ND}(t_k) = \mathbb{E}(\overline{P_n^{ND}}) = \sum_{i=1}^{4} x_{n,i}(t_k)\overline{P_{n,i}^{ND}} \tag{10}$$

It is desired to know how $\mathbb{P}_n^D(t_k)$ degrades over time. Let $\mathbb{P}_n^D(t_0)$ be the reference to measure the degradation. The following metric called capacity degradation from time t_0 to t_k is introduced:

$$\delta_n^D(t_k) = \mathbb{P}_n^D(t_0) - \mathbb{P}_n^D(t_k) \tag{11}$$

Similarly, the capacity degradation for non-dispatchable sources is computed by

$$\delta_n^{ND}(t_k) = \mathbb{P}_n^{ND}(t_0) - \mathbb{P}_n^{ND}(t_k) \tag{12}$$

Dispatchable components are discriminated from non-dispatchable ones because the degradation of non-dispatchable DERs is considered uncontrollable by EM, while dispatchable components are considered controllable.

3.4. Reconfigure EM's optimization problem

EM is briefly discussed in Section 2 and mathematically presented in a general manner in (1). As discussed earlier, EM allocates power generation and delivery to the grid's components to gain economic benefits; it decides operating conditions for these units, and thus it impacts the components' degradation processes as described in (7). By adjusting the configuration of EM's optimization problem, the components' operating conditions can be adjusted; thus, it impacts the components' degradation processes. There are two strategies to adjust the operating conditions of components through EM. The first strategy is adjusting the components' generating or transferring maximum capacities, and the second one is adjusting the EM's objective function.

The first strategy to change the operating condition of a component through EM is adjusting the maximum capacity. The constraint $\mathbf{P}_n^D \in C^{\mathbf{P}^D}$ in (1b) is typically a box constraint as

$$\underline{P_n^D} \le P_n^D \le \overline{P_n^D} \tag{13}$$

The expression (13) is understood as a dispatchable source that has a lower and an upper limit on power generation or transfer. Reducing $\overline{P_n^D}$ likely reduces the component's operating condition as EM will respect the limit in its optimization process. However, in doing so, it reduces the system's capability to meet load demand, especially when load demand is at a peak; hence it reduces system reliability. Therefore, this work follows the second strategy that additional costs considering degradation costs are added.

EM mainly considers the economic curves of the components. Recently, components' degradation has been received more concerns. There is work adding components' degradation costs into the EM's objective function [11,39]. Specifically, in [39], a linear degradation cost is added to the EM's objective function. Additionally, in [11], the degradation rate of a component is estimated from empirical data, and it is input into an economic model considering degradation, investment, and fuel consumption costs to construct an objective cost for a component.

Now the additional cost added to $f_n^{eco}(P_n^D)$ in (1) is discussed. The objective is to reduce the total components' degradation costs. In the previous section, the capacity degradation metric $\delta_n^D(t_k)$ for a dispatchable energy source is introduced in (12). Let C_n^D be the capital cost of the dispatchable component at bus n. Suppose the capital cost is linearly proportional to its maximum capacity. The degradation cost c_n^D of component n from t_0 to t_K can be estimated as

$$c_n^D = \delta_n^D(t_K) * C_n^D * \frac{1}{1-\rho_3} \tag{14}$$

The term $\frac{1}{1-\rho_3}$ is included in the above Eq. (14) because a replacement is considered for a component entering state 4. Let $P_n^{*D}(t_k)$ be the optimized power generation of a dispatchable component at bus n at t_k with the current cost function. The average degradation cost for each power unit is

$$\Delta_n^D(t_K) = \frac{c_n^D}{\sum_{k=0}^{K} P_n^{*D}(t_k)} \tag{15}$$

Table 1
Component list.

No.	Region	Bus	Technology	Capacity (kW)	CAPEX ($)
1	1	1	Transformer	4000	30,800
2	1	4	Wind turbine	1500	2,625,000
3	2	8	Microturbine	400	1,032,000
4	2	6	Solar	200	552,000
5	3	14	Microturbine	200	516,000
6	3	18	Solar	200	552,000
7	4	20	Microturbine	200	516,000
8	4	22	Solar	200	552,000
9	5	24	Microturbine	400	1,032,000
10	5	25	Solar	500	1,380,000
11	6	30	Microturbine	400	1,032,000
12	6	32	Solar	200	552,000

The EM's objective function is updated as

$$f(\mathbf{P}^D) = \sum_{n\in D}\left(f_n^{eco}(P_n^D) + \Delta_n^D(t_K)P_n^D\right) \tag{16}$$

4. Numerical simulation

4.1. System description

The proposed framework is validated by numerical simulations on a personal computer in this section. The IEEE 33 bus system in [40] with additions of DERs is used to validate the proposed scheme. This system consists of 33 buses and 32 lines, and it has a voltage of 12.66 kV. The system is geographically divided into 6 regions, with each corresponding to an Energy Management (EM) agent. MTs are deployed as dispatchable energy sources in the system, and WT and PV systems are added as non-dispatchable sources. The locations, rated power, and generation technologies of the DERs are shown in Table 1.

4.2. Data preparation

4.2.1. Components' CAPEX

Components' capital expenditure (CAPEX) is used to estimate their degradation costs. CAPEX typically includes equipment costs and installation costs. An investigation to obtain the prices of the considered components is carried out in this work. The WT technology costs between $1,300,000 and $2,200,000 for each MW capacity [41], the cost of each kW capacity is $2580 for MT technology [42], and $2760 for PV technology [43]. In addition, a transformer in the range of 4 MVA generally costs $30,800 [44]. With those unit prices, initial investment costs of DERs are calculated to match their capacities and are shown in Table 1.

4.2.2. Degradation data

Because degradation data is usually kept confidential by utilities, notional data is generated by the Wiener process, which has been widely used to model degradation behaviors of an engineering system [45,46]. Mathematically, the Wiener-process-based degradation model is expressed as

$$d(t) = \iota t + \nu B(t) \tag{17}$$

where $d(t)$ is the degradation signal at time t, ι is the drift coefficient, $\nu > 0$ is the diffusion coefficient, and $B(t)$ is the standard Brownian motion. The stochastic dynamics of the degradation process is presented by the Brownian motion. Degradation signal data can be generated by the above model if the parameters ι and ν are known. In this application context, ι relates to degradation rate, and ν relates to noises.

It is shown in [42] that an MT is expected to function between 40,000 h and 80,0000 h. Assuming the minimum degradation rate is associated with 40,000 h of operation and 80,000 h of operations makes microturbines have the maximum degradation rate. Suppose a replacement is considered for an MT when its capacity's degradation reaches 80%, then the minimum degradation rate can be estimated at around 2.19 %/year, and the maximum degradation rate is around 4.38 %/year. It is reported in [47] that the wind turbine degradation rate has a range of $[1.4, 1.8]$ %/year. In [48], the degradation rate of a transformer with high-water content in the winding paper is reported to be in the range of [1.5,3.0] %/year. In [49], the degradation rate of a PV plant is reported in the range of [0.8,1.2] %/year. Table 2 shows the degradation rates of power generation and delivery technologies used in this work. With data in the table, each minimum or maximum degradation rate is used to generate 30 degradation paths. The generated data is used to obtain the minimum degradation intensity matrix $\underline{\lambda} = [\underline{\lambda_{ij}}]_{4\times4}$ by Algorithm 1. In Algorithm 1, Y is the number of generated degradation paths, and d_y is a degradation path, which is an array. S_y is an array storing the state of all elements of d_y. The algorithm is used to compute the transition probability from state i to state j. Similarly, the maximum degradation intensity matrix $\overline{\lambda} = [\overline{\lambda_{ij}}]_{4\times4}$ can be obtained.

Table 2
Degradation rate.

No.	Technology	Max. Degradation Rate %/year	Min. Degradation Rate %/year
1	Transformer	1.5	3.0
2	MT	2.19	4.38
3	WT	1.4	1.6
4	PV	0.8	1.2

Algorithm 1 Training minimum degradation intensity matrix

1. Input: Degradation paths $d_y, y \in \{1, \dots, Y\}$
2. Initialize: $\underline{\lambda} = [0]_{4\times4}$
3. **for** $y := 1$ *to* Y **do**
    - Assign state for $d_y(1)$: $S_y(1) = i$, i=1 or i=2 or i=3 or i=4
    - **for** $l := 2$ *to* $length(d_y) - 1$ **do**
        - Assign state for $d_y(l)$: $S_y(l) = i$, i=1 or i=2 or i=3 or i=4
        - $\underline{\lambda}(S_y(l-1), S_y(l)) = \underline{\lambda}(S_y(l-1), S_y(l)) + 1$
    - **end**

end

4. Normalize $\underline{\lambda}$
5. **return** $\underline{\lambda}$

4.2.3. Operating data

The proposed degradation model in (7) is load-dependent, and the time step is 1 h. Therefore, the information of hourly load and non-dispatchable power generation is needed to run the model. Residential load profiles, EV charging profiles, wind speed, solar irradiance, and temperature are stochastically generated probabilistic models. While residential load profiles, solar irradiance, and temperature are generated using the CREST model in [50], EV charging profiles are generated by the new methodology presented in [26]. Because the CREST model does not consider wind, wind speed data is simply generated by the Weibull distribution. Non-dispatchable renewable power generation data such as wind power generation and solar power generation is estimated using maximum power point tracking (MPPT) models Fig. 4 shows load profile data generated, and Fig. 5 shows non-dispatchable power generation data generated for a day. It is noted that the models can generate data for all days in a year.

4.3. Numerical simulation results and discussion

Three test cases are carried out, and simulation results are discussed.

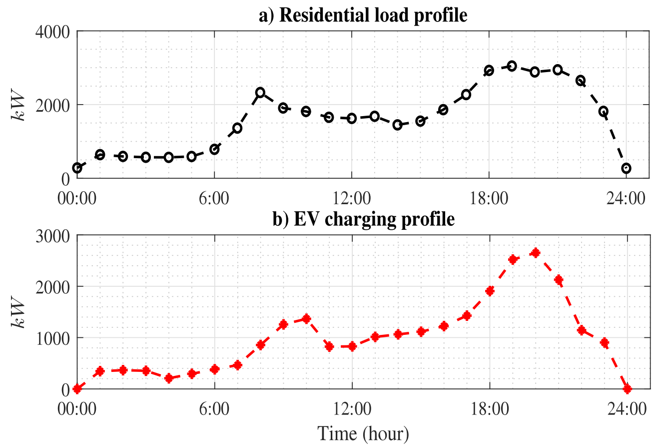

Fig. 4. Load profile for a day: (a) Residential load profile (b) EV charging profile.

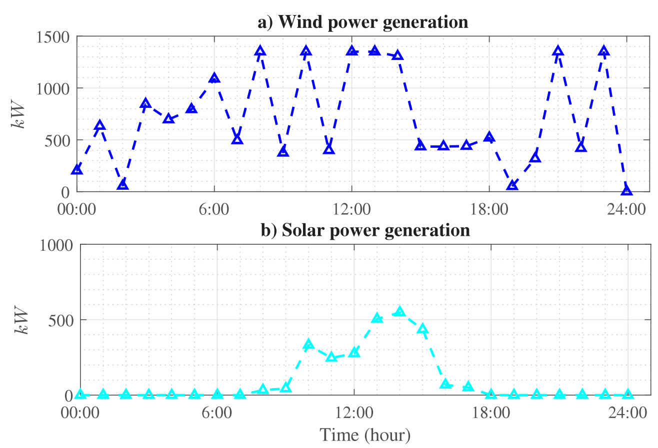

Fig. 5. Non-dispatchable power generation for a day: (a) Wind power generation (b) Solar power generation.

4.3.1. Case 1

The EM's objective functions do not consider degradation costs. The main purpose of this testing case is to see the degradation costs within 30 days of operating the system. The degradation costs in 30 days of the components listed in Table 1 are estimated with three scenarios: (1) all the components start at state 1, (2) all the components start at state 2, and (3) all the components start at state 3. Degradation data is generated by the method described in Section 4.2.2, and the degradation rates used are in Table 2. The generated data is used to train the Markov degradation prediction model, which is implementing Algorithm 1. Fig. 6 shows the simulation results. As can be seen in the figure, the total degradation cost for the dispatchable-source components is around $47.000, and that of non-dispatchable-source components is around $27.000. The objective of the proposed DFAF is to reduce the total degradation cost for the dispatchable-source components, which is shown next testing cases in which three test cases are carried out.

4.3.2. Case 2

Data used to train the Markov model is generated using degradation rates on Table 2. Figs. 7 and 8 show simulation results. As can be seen in Fig. 7, the degradation of components 3, 5, 7, 9, and 11 are abated at the expense of component 1. This is because the CAPEX of the MTs is more expensive than the transformer, while the degradation rates of the MTs are lower. Fig. 8 shows the cost savings of deploying DFAF compared to the case without DFAF. The proposed strategy saves

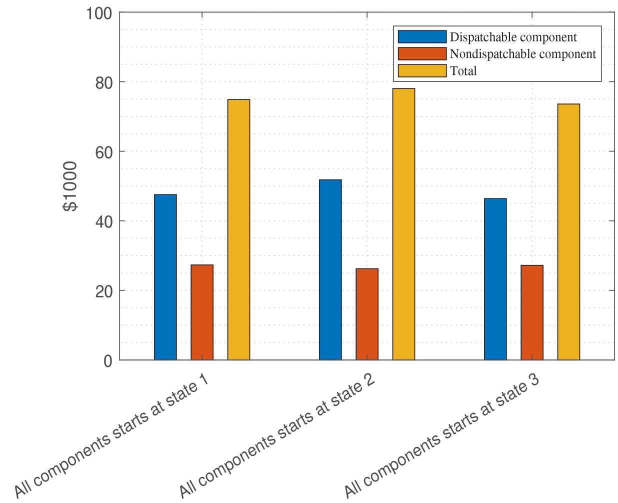

Fig. 6. Case 1: Degradation cost in 30 days.

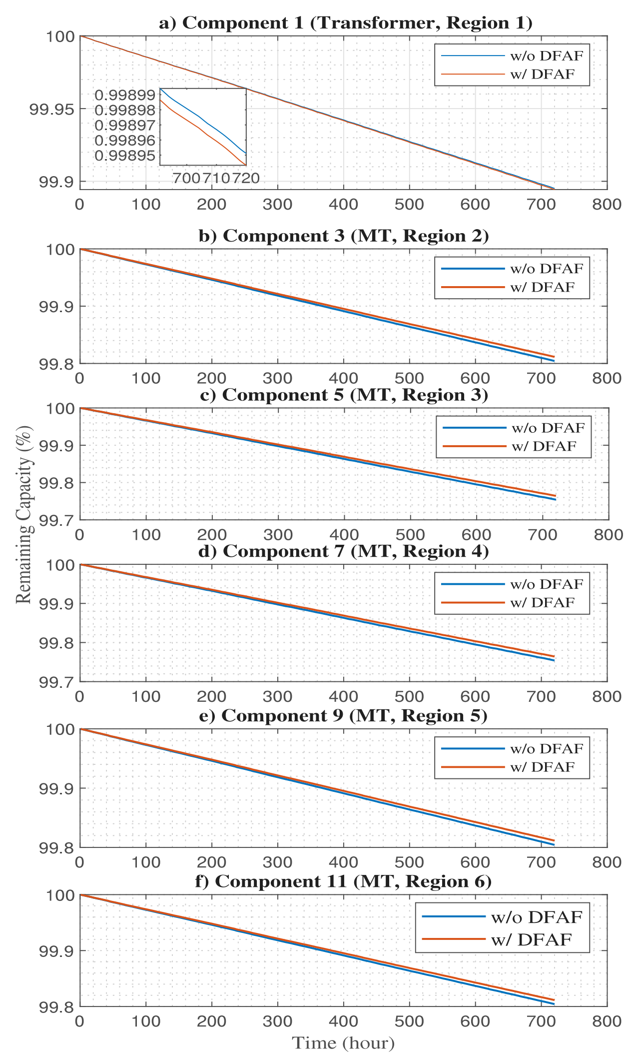

Fig. 7. Case 2: The degradation of the components with and without DFAF.

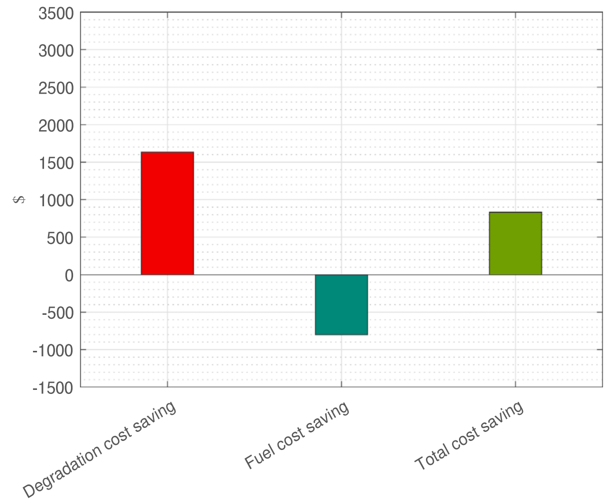

Fig. 8. Case 2: Cost savings with DFAF.

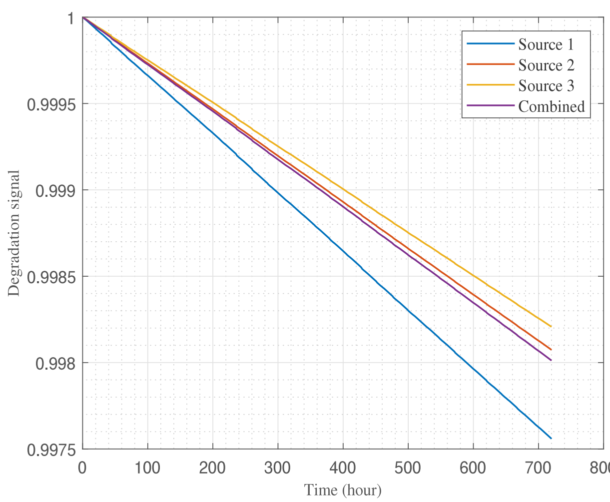

Fig. 9. Case 3: Predicted degradation of component 3.

≈ \$1634 for the total degradation cost, but the system spends ≈ \$802 more on fuel consumption. However, the total saving is ≈ \$832.

4.3.3. Case 3

In this case, the effectiveness of ET in fusing multiple sources of information is shown. In the previous cases, data used to train the Markov model is generated using degradation rates on Table 2. In this case, for component 3, two data sets are generated using the degradation rates on Table 2, which are called source 2 and source 3, another data set is generated by using degradation range [2.9200,5.8400] %/year, which is called source 1. Suppose source 1 is an unreliable source. As can be seen in Fig. 9, the ET's combination can discern the unreliability of source 1 as the combined result is closer to source 2 and source 3 compared to source 1.

5. CHIL experimentation

The proposed strategy is realized by a CHIL experimentation on the IEEE 33 bus system described in Section 4.1. Equipment in Real-time COtrol and Optimization Laboratory (RT-COOL) at Clemson University is used to construct an ADMS with the degradation forecasting functionality integrated with EM. The main purpose of the CHIL implementation with the laboratory equipment are to show real-time implementation feasibility and its synergic to other layers of the ADMS. Next, the details of the CHIL implementation and experimental results are presented.

5.1. System modeling

The IEEE 33 bus system is simulated by the MATLAB/Simulink software. Rowen's model is used to simulate MTs' engines [51], and the control structure in [52] is applied to integrate the MTs with the grid through power electronics converters. Furthermore, the type 4 WT model in [53] is used. Additionally, PV panels are modeled by the double-diode model with parameters extracted from the Siemens SM50 solar panel's specifications. Both the WT and PV systems have MPPT modules to obtain optimal generation. Average models are used for power electronics converters. The model is later compiled into the C++ programming language by OPAL-RT Technologies's RT-LAB software, and the compiled program is deployed into a digital real-time simulator (DRTS) OPAL-RT OP4510. Average models are used to model DERs instead of detailed models because the DRTS has limited computational power to run detailed models of all the DERs in real time. However, average models are sufficient enough to demonstrate the DFAF strategy. The sampling time used in this work is 80 μs. The MATLAB/Simulink program is shown in Fig. 10.

For the sake of simplicity, the degradation processes of the system's components are modeled by the Wiener process included in the MATLAB/Simulink model to generate degradation signals. Those degradation signals are sent to the controller, which implements the DF function, which is discussed in the next subsection. Additionally, PM is a decentralized strategy receiving references from EMs to control DERs to follow, and it is also embedded into the MATLAB/Simulink model.

5.2. Integrating degradation forecasting into ADMS

It is noted that the EM strategy and its CHIL implementation are discussed detailedly in [14]. Briefly, each region has an EM to manage the region in collaboration with other EMs in a distributed manner. The EM strategy is realized by the LabVIEW software, and then it is deployed into 6 real-time controllers NI sbRIO 9627. This work inherits the EM system and extends the work by adding the proposed DF layer.

The proposed DF strategy is realized in the LabVIEW environment and deployed into a real-time NI sbRIO 9627 controller. The time step for DF is 1 h. Every 1 h, the controller receives degradation signals sent from the DRTS. The degradation signals are converted to probabilities of the four states as the initial state $\mathbf{x}_n(t_0)$ for the Markov chain based prediction model discussed in Section 3.1. There is a computer playing as a server is added. The MATLAB script module in LabVIEW is used to implement the server's functionalities. These functionalities are described now. First, the server stores data and trains the data using Algorithm 1 to obtain the maximum and minimum degradation intensity matrices for each source of information. Second, the server will send trained models whenever the real-time controller, which implements the DF, queries for the models. Third, the server will respond to the real-time controller's query for predicted power generation or delivery. The DF controller, in collaboration with the server, runs the Markov chain degradation model presented in Section 3.1.2. It predicts the degradation paths of the components in 30 days with 1-hour data resolution, then it computes the degradation costs discussed in Section 3.4 to send to EM. A 1 GB erthernet communication network is established for the real-time controllers and the DRTS to communicate.

There is also a human-machine interface (HMI) added to monitor the system, and an NI sbRIO 9627 real-time controller board is set up for this function. The HMI collects operating data from the DRTS, the EM controllers, and the DF controller, and then it displays them on a monitor. There are five main displaying screens. First, the Control screen has start/stop buttons to control the experimentation, and it also has inputs for the CHIL system's information, such as controllers' IP addresses. Second, the System Monitoring screen displays components'

Fig. 10. MATLAB/Simulink model of the IEEE 33 bus system.

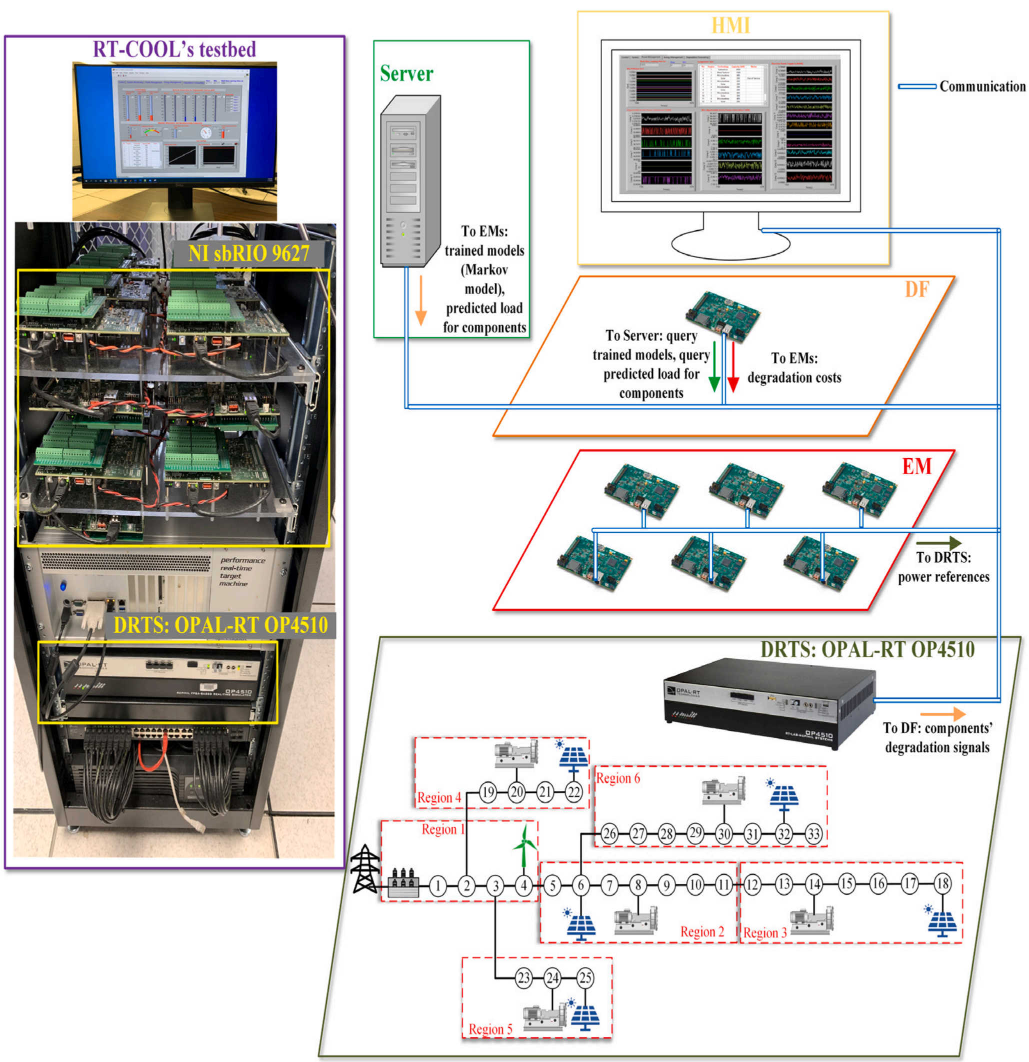

Fig. 11. CHIL Implementation.

statuses with the grid diagram. Third, the Power Management screen shows bus voltages, measured active and reactive power from DERs, and the substation transformer. Fourth, the Energy Management screen is to show weather information, non-dispatchable power generation, load demand, optimal power generation and delivery of dispatchable sources. Finally, the Degradation Forecasting displays the degradation signals received from the model running in the DRTS and the degradation predictions of the grid's components. Fig. 12 shows the System

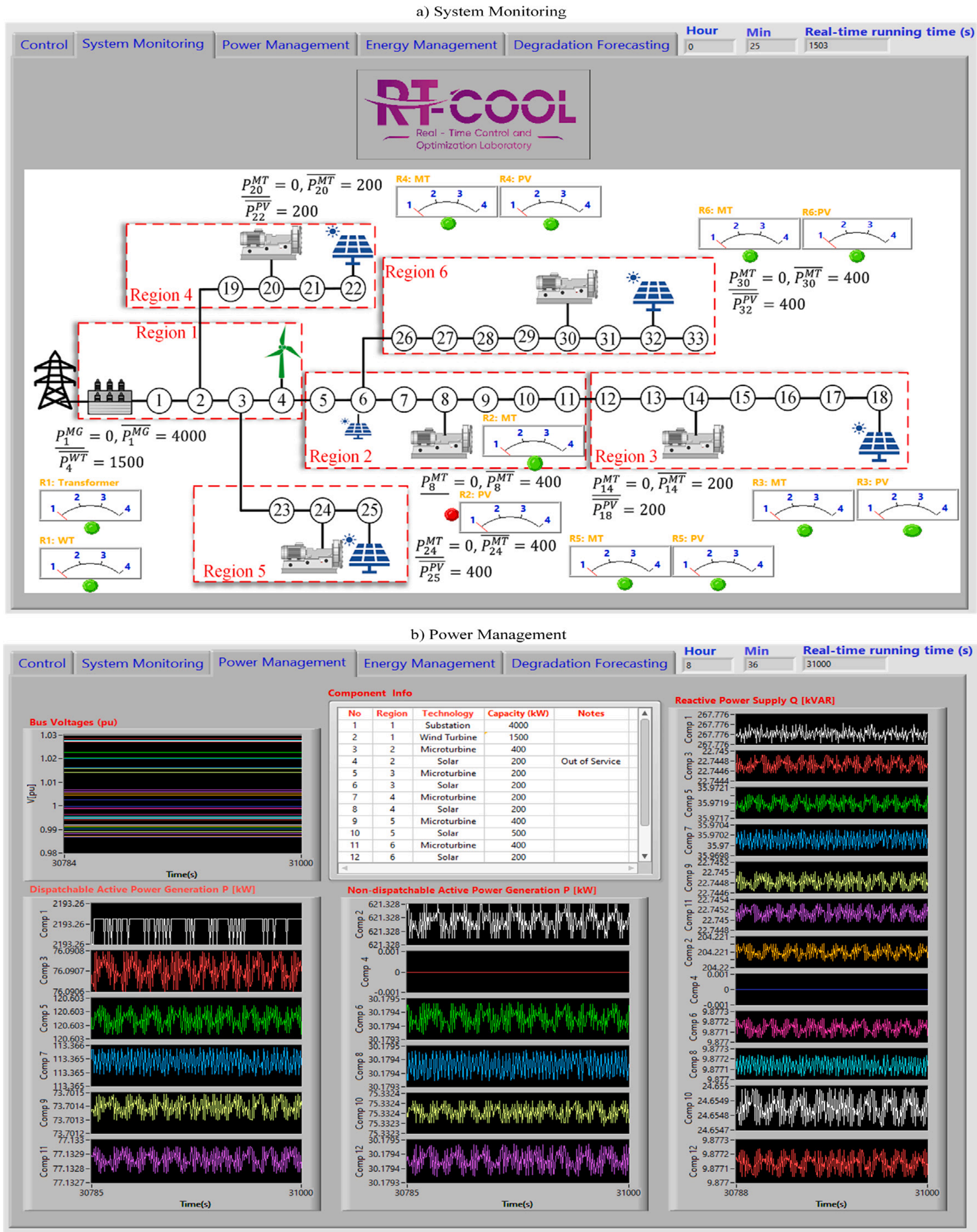

Fig. 12. HMI display: (a) System Monitoring screen (b) Power Management screen.

Monitoring and Power Management screens. Fig. 13 shows the Energy Management and Degradation Forecasting screens.

5.3. Experimental results

The constructed CHIL system described in Fig. 11 is run, and the three layers PM, EM, and DF work synergically. As can be seen in Fig. 13 (b), degradation signals are sent from the model to HMI running in the DRTS for displaying. It is noted that component 4 is out of service; therefore, the degradation signal is zero. On the left side of the figure, it shows the predicted degradation paths of the components. To show the effectiveness of the proposed strategy, the server is requested to compute the costs saved by the strategy. As can be in the middle of the figure, DFAF saves ≈ \$1634 in degradation costs in 30 days. However, the fuel cost increases by ≈ \$802 because the EM's objective function is adjusted. But overall, the proposed strategy saves ≈ \$832 for the system. The experimental results match the numerical simulations.

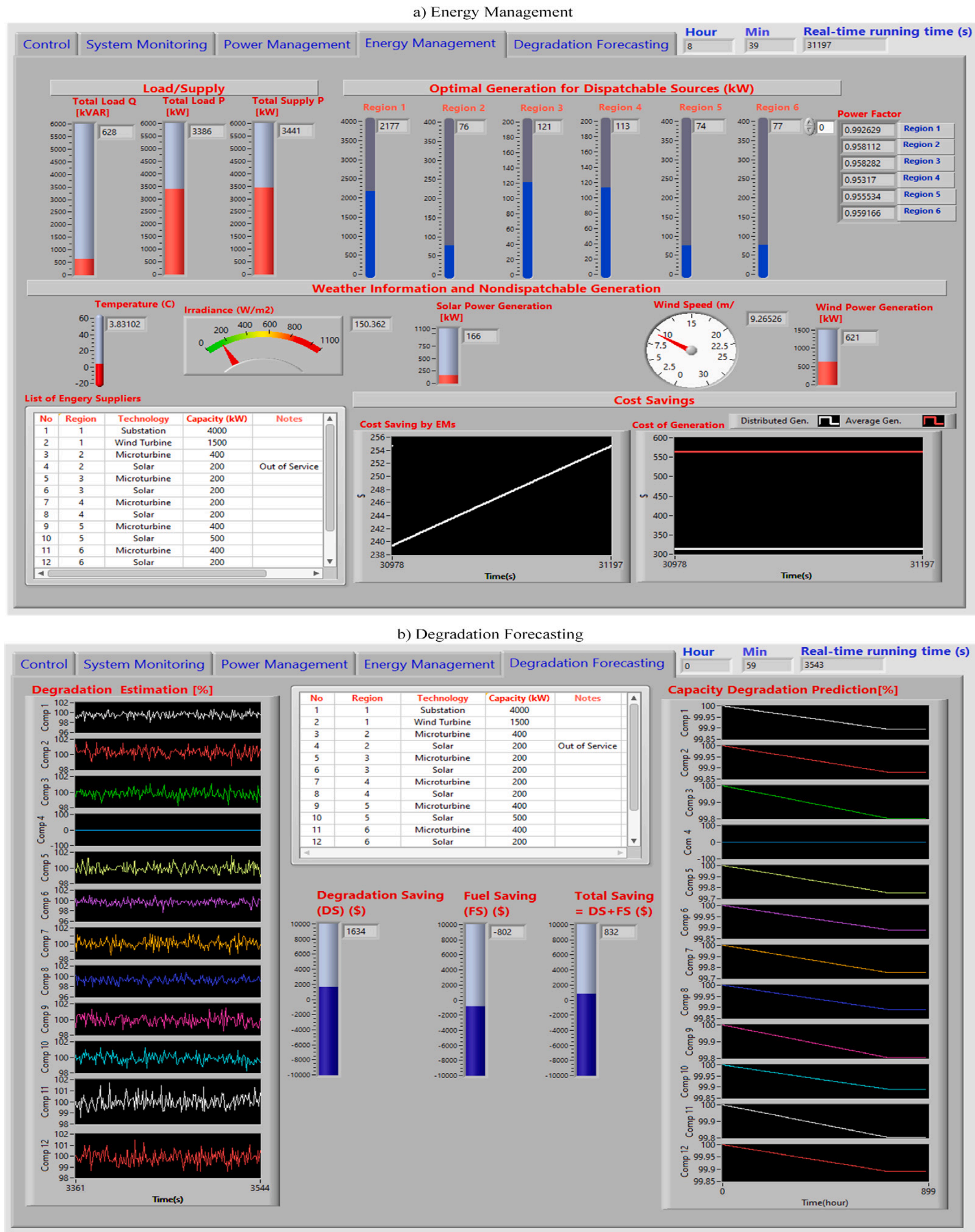

Fig. 13. HMI display: (a) Energy Management screen (b) Degradation Forecasting screen.

6. Conclusion and future work

This paper proposes a DFAF and its integration into the existing hierarchical ADMS as an upper layer to EM to abate the degradation processes of components to reduce operating costs. A Markov chain-based degradation model is constructed to predict the degradation paths of a grid's components in which components' states are modeled by a multi-state model. It is a load-dependent degradation model reasoning from observations of considered DERs' degradation behaviors. Multiple sources of data can be used to train the Markov prediction model that ET is used to combine predicted results to enhance the reliability of the prediction model. The predicted results are used to adjust EM, which is a component of the ADMS concept, to abate the degradation of components with higher degradation costs. The proposed strategy is verified on the IEEE 33 bus system by numerical simulations. In addition, CHIL experimentation for the proposed scheme is implemented with laboratory equipment. Both numerical simulations and CHIL experimentation show operation cost savings for the studied system.

There are research directions that can extend this work, for example:

- First, the proposed framework can be applied to other types of electrical systems, such as hybrid electric vehicles (HEVs).
- Second, integrating optimal maintenance planning with forecasting results into the framework is another direction.
- Third, investigating the impact of load modeling could be a future research direction for this work.
- Fourth, the proposed framework can be used to investigate other forecasting methods.

CRediT authorship contribution statement

Phuong H. Hoang: Methodology, Software, Investigation, Writing – original draft, Visualization. **Gokhan Ozkan:** Software, Writing – review & editing. **Payam Ramezani Badr:** Software, Writing – review & editing. **Laxman Timilsina:** Software, Writing – review & editing. **Behnaz Papari:** Software, Writing – review & editing. **Christopher S. Edrington:** Writing – review & editing, Supervision, Project administration.

Declaration of competing interest

The authors declare that they have no known competing financial interests or personal relationships that could have appeared to influence the work reported in this paper.

Data availability

Data will be made available on request.

References

[1] Aguero JR, Takayesu E, Novosel D, Masiello R. Modernizing the grid: Challenges and opportunities for a sustainable future. IEEE Power Energy Mag 2017;15(3):74–83.

[2] National Renewable Energy Laboratory. Insights into advanced distribution management systems. 2015, Voices of Experience-U.S. Department of Energy-Office of Electricity Delivery & Energy Reliability.

[3] Sun X, Chavali RVK, Alam MA. Real-time monitoring and diagnosis of photovoltaic system degradation only using maximum power point—The Suns-Vmp method. Prog Photovolt, Res Appl 2019;27(1):55–66. http://dx.doi.org/10.1002/pip.3043.

[4] Jia X, Jin C, Buzza M, Wang W, Lee J. Wind turbine performance degradation assessment based on a novel similarity metric for machine performance curves. Renew Energy 2016;99:1191–201. http://dx.doi.org/10.1016/j.renene.2016.08.018.

[5] Hoang PH, Ozkan G, Badr PR, Edrington CS, Papari B. An online degradation forecasting and abatement framework for hybrid electric vehicles. SAE Tech Pap 2021;(2021):1–6. http://dx.doi.org/10.4271/2021-01-0161.

[6] Office of Electricity Delivery and Energy Reliability, Department of Energy. Voices of experience | insights into advanced distribution management systems. IEEE Trans Smart Grid 2015.

[7] Vu TV, Gonsoulin DE, Diaz F, Edrington CS, El-mezyani T. Predictive control for energy management in ship power systems under high-power ramp rate loads. IEEE Trans Energy Convers 2017;32:788–97.

[8] Guerrero JM, Vasquez JC, Matas J, de Vicuna LG, Castilla M. Hierarchical control of droop-controlled AC and DC microgrids—A general approach toward standardization. IEEE Trans Ind Electron 2011;58(1):158–72. http://dx.doi.org/10.1109/TIE.2010.2066534.

[9] Sun Y. Operational reliability assessment of power systems considering condition-dependent failure rate. IET Gener Transm Distrib 2010;4:60–72, (12), [Online]. Available: https://digital-library.theiet.org/content/journals/10.1049/iet-gtd.2009.0006.

[10] Emsley AM, Stevens GC. Review of chemical indicators of degradation of cellulosic electrical paper insulation in oil-filled transformers. IEE Proc: Sci Measur Technol 1994;141(5):324–34. http://dx.doi.org/10.1049/ip-smt:19949957.

[11] Cuneo A, Zaccaria V, Tucker D, Traverso A. Probabilistic analysis of a fuel cell degradation model for solid oxide fuel cell and gas turbine hybrid systems. Energy 2017;141:2277–87. http://dx.doi.org/10.1016/j.energy.2017.12.002.

[12] Hoang PH, Ozkan G, Deb N, Edrington CS, Papari B. An evidence theory based advisory layer for all-electric ship power systems. In: 2019 IEEE electric ship technologies symposium. 2019, p. 599–604. http://dx.doi.org/10.1109/ESTS.2019.8847884.

[13] Olsson T, Ramentol E, Rahman M, Oostveen M, Kyprianidis K. A data-driven approach for predicting long-term degradation of a fleet of micro gas turbines. Energy AI 2021;4:100064. http://dx.doi.org/10.1016/j.egyai.2021.100064.

[14] Richardson RR, Osborne MA, Howey DA. Gaussian process regression for forecasting battery state of health. J Power Sources 2017;357:209–19. http://dx.doi.org/10.1016/j.jpowsour.2017.05.004.

[15] Mathew MS, Kandukuri ST, Omlin CW. Estimation of wind turbine performance degradation with deep neural networks. In: PHM society European conference. 2022, p. 351–9.

[16] Djurdjanovic D, Lee J, Ni J. Watchdog agent - An infotronics-based prognostics approach for product performance degradation assessment and prediction. Adv Eng Inform 2003;17(3–4):109–25. http://dx.doi.org/10.1016/j.aei.2004.07.005.

[17] Hoang PH, Badr PR, Ozkan G, Edrington CS, Papari B. Integrating degradation forecasting into control and management system of DC microgrids. In: 2021 IEEE fourth international conference on DC microgrids. 2021, p. 1–6.

[18] Hoang PH, Ozkan G, Badr PR, Edrington CS, Timilsina L. A prognostic based control framework for hybrid electric vehicles. SAE Tech Pap 2022;1–6.

[19] Ciftci O, Mehrtash M, Kargarian A. Data-driven nonparametric chance-constrained optimization for microgrid energy management. IEEE Trans Ind Inf 2020;16(4):2447–57.

[20] Kanchev H, Lu D, Colas F, Lazarov V, Francois B. Energy management and operational planning of a microgrid with a PV-based active generator for smart grid applications. IEEE Trans Ind Electron 2011;58(10):4583–92.

[21] A multi-agent system for energy management of distributed power sources. Renew Energy 2010;35(1):174–82.

[22] Papari B, Edrington CS, Bhattacharya I, Radman G. Effective energy management of hybrid AC–DC microgrids with storage devices. IEEE Trans Smart Grid 2019;10(1):193–203.

[23] Papari B, Edrington CS, Gonsoulin D. Optimal energy-emission management in hybrid AC-DC microgrids with vehicle-2-grid technology. J Renew Sustain Energy 2019;11(1).

[24] Papari B, Edrington CS, Vu TV, Diaz-Franco F. A heuristic method for optimal energy management of DC microgrid. In: 2017 IEEE second international conference on DC microgrids. 2017, p. 337–43. http://dx.doi.org/10.1109/ICDCM.2017.8001066.

[25] Mühlpfordt T, Dai X, Engelmann A, Hagenmeyer V. Distributed power flow and distributed optimization—Formulation, solution, and open source implementation. Sustain Energy Grids Netw 2021;26.

[26] Hoang PH, Ozkan G, Badr PR, Papari B, Edrington CS, Zehir MA, et al. A dual distributed optimal energy management method for distribution grids with electric vehicles. IEEE Trans Intell Transp Syst 2022;23:13666–77.

[27] Najjar YS, Alalul OF, Abu-Shamleh A. Degradation analysis of a heavy-duty gas turbine engine under full and part load conditions. Int J Energy Res 2020;44(6):4529–42. http://dx.doi.org/10.1002/er.5229.

[28] Li Z, Xu T, Gu J, Dong Q, Fu L. Reliability modelling and analysis of a multi-state element based on a dynamic bayesian network. R Soc Open Sci 2018;5(4). http://dx.doi.org/10.1098/rsos.171438.

[29] Lisnianski A, Elmakias D, Laredo D, Ben Haim H. A multi-state Markov model for a short-term reliability analysis of a power generating unit. Reliab Eng Syst Saf 2012;98(1):1–6. http://dx.doi.org/10.1016/j.ress.2011.10.008.

[30] Akay B, Ragni D, Ferreira CS, Bussel GJWV. Investigation of the root flow in a horizontal axis. Wind Energy 2013;(May 2015):1–20. http://dx.doi.org/10.1002/we.

[31] Tu Tran QT, Davies K, Roose L, Doan BV, Nguyen NQ. Online distribution service transformer health assessment using real-time grid energy monitor. In: 2020 IEEE Kansas power and energy conference. 2020, p. 2–7. http://dx.doi.org/10.1109/KPEC47870.2020.9167580.

[32] Igie U, Diez-Gonzalez P, Giraud A, Minervino O. Evaluating gas turbine performance using machine-generated data: Quantifying degradation and impacts of compressor washing. J Eng Gas Turb Power 2016;138(12):1–18. http://dx.doi.org/10.1115/1.4033748.

[33] Wymore ML, Van Dam JE, Ceylan H, Qiao D. A survey of health monitoring systems for wind turbines. Renew Sustain Energy Rev 2015;52(1069283):976–90. http://dx.doi.org/10.1016/j.rser.2015.07.110.

[34] Hanachi H, Liu J, Banerjee A, Chen Y. A framework with nonlinear system model and nonparametric noise for gas turbine degradation state estimation. Meas Sci Technol 2015;26(6). http://dx.doi.org/10.1088/0957-0233/26/6/065604.

[35] Jordan DC, Deline C, Kurtz SR, Kimball GM, Anderson M. Robust PV degradation methodology and application. IEEE J Photovolt 2018;8(2):525–31. http://dx.doi.org/10.1109/JPHOTOV.2017.2779779.

[36] Ye JY, Reindl T, Aberle AG, Walsh TM. Effect of solar spectrum on the performance of various thin-film PV module technologies in tropical Singapore. IEEE J Photovolt 2014;4(5):1268–74. http://dx.doi.org/10.1109/JPHOTOV.2014.2328585.

[37] Billinton R, Allan RN. Reliability evaluation of power systems. 2nd ed.. New York and London: Plenum Press; 1996.

[38] Shafer G. A mathematical theory of evidence. NJ: Princeton University Press; 1976.

[39] Shi Z, Liang H, Huang S, Dinavahi V. Distributionally robust chance-constrained energy management for islanded microgrids. IEEE Trans Smart Grid 2019;10(2):2234–44. http://dx.doi.org/10.1109/TSG.2018.2792322.

[40] Baran ME, Wu FF. Network reconfiguration in distribution systems for loss reduction and load balancing. IEEE Trans Power Deliv 1989;4(2):1401–7.

[41] Windustry. How much do wind turbines cost?. 2021, [Online]. Available: https://www.windustry.org/how_much_do_wind_turbines_cost.

[42] Ezekiel Enterprises LLC. Microturbine generators. 2021, Ezekiel Enterprises Continuing Education for Licensed Professional Engineers, [Online]. Available: https://cdn.ez-pdh.com/course-material/EE1285-Microturbine-Generators.pdf.

[43] Energy Sage. How much does a solar panel installation cost? 2021, https://www.energysage.com/, [Online]. Available: https://news.energysage.com/how-much-does-the-average-solar-panel-installation-cost-in-the-u-s/.

[44] Alibabacom. 2021, Alibaba.Com, [Online]. Available: https://www.alibaba.com/product-detail/Price-for-35kv-5000-kva-4_1600289293351.html?spm=a2700.pc_countrysearch.main07.8.16087df8lGkPFX.

[45] Si XS, Wang W, Hu CH, Chen MY, Zhou DH. A Wiener-process-based degradation model with a recursive filter algorithm for remaining useful life estimation. Mech Syst Signal Process 2013;35(1–2):219–37. http://dx.doi.org/10.1016/j.ymssp.2012.08.016.

[46] Wang X. Wiener processes with random effects for degradation data. J Multivariate Anal 2010;101(2):340–51. http://dx.doi.org/10.1016/j.jmva.2008.12.007.

[47] Staffell I, Green R. How does wind farm performance decline with age? Renew Energy 2014;66:775–86. http://dx.doi.org/10.1016/j.renene.2013.10.041, [Online]. Available: https://www.sciencedirect.com/science/article/pii/S0960148113005727.

[48] T&D World. How transformers age. 2019, https://Www.Tdworld.Com/, [Online]. Available: https://www.tdworld.com/substations/article/20972255/how-transformers-age.

[49] Bolinger M, Gorman W, Millstein D, Jordan D. System-level performance and degradation of 21 GWDC of utility-scale PV plants in the United States. J Renew Sustain Energy 2020;12.

[50] Richardson I, Thomson M, Infield D, Clifford C. Domestic electricity use: A high-resolution energy demand model. Energy Build 2010;42(10):1878–87.

[51] Rowen WI. Simplified mathematical representations of heavy-duty gas turbines. J Eng Power 1983;105(4):865–9.

[52] Grillo S, Massucco S, Morini A, Pitto A, Silvestro F. Microturbine control modeling to investigate the effects of distributed generation in electric energy networks. IEEE Syst J 2010;4(3):303–12.

[53] Hansen AD, Margaris ID. Type IV wind turbine model. 2014, DTU Wind Energy.